Hydrologic Control on Arsenic Cycling at the Groundwater-surface Water Interface of a Tidal Channel

*Xuan Yu [a, b], Joshua J. LeMonte [c], Junxia Li [d], Jason W. Stuckey [e], Donald L. Sparks [f], John G. Cargill [g], Christopher J. Russoniello [h], Holly A. Michael [i,]**

[a] *Center for Water Resources and Environment, School of Civil Engineering, Sun Yat-sen University, Guangzhou, 510275, China https://orcid.org/0000-0002-9055-7923*

[b] *Southern Marine Science and Engineering Guangdong Laboratory (Zhuhai), Zhuhai, 519082, China*

[c] *Department of Geological Sciences, Brigham Young University, Provo, UT 84602, United States*

[d] *School of Environmental Studies & State Key Laboratory of Biogeology and Environmental Geology & Key Laboratory of Source Apportionment and Control of Aquatic Pollution, Ministry of Ecology and Environment, China University of Geosciences, Wuhan, 430074, China*

[e] *Department of Natural Sciences and Environmental Science Program, Multnomah University, Portland, OR 97220, United States*

[f] *Department of Plant and Soil Sciences, University of Delaware, Newark, DE 19716, United States*

[g] *Department of Natural Resources and Environmental Control, New Castle, DE 19720, United States*

[h] *Department of Geosciences, University of Rhode Island, Kingston, RI 02881, United States*

[i] *Department of Earth Sciences and Department of Civil & Environmental Engineering, University of Delaware, Newark, DE 19716, United States* https://orcid.org/0000-0003-1107-7698

*Email: hmichael@udel.edu

KEYWORDS: Arsenic, redox, hydrogeochemistry, groundwater–surface water interaction, tide, industrial contamination.

Synopsis

This study reports enrichment of arsenic in the bank of a tidal channel controlled by multi-scale hydrologic shifts. Our field observation reveals arsenic contamination risk in different hydrologic regimes.

Accepted Manuscript
Version of record at: https://doi.org/10.1021/acs.est.2c05930

ABSTRACT

Historical industrial activities have resulted in soil contamination at sites globally. Many of these sites are located along coastlines, making them vulnerable to hydrologic and biogeochemical alterations due to climate change and sea-level rise. However, the impact of hydrologic dynamics on contaminant mobility in tidal environments has not been well studied. Here we collected data from pressure transducers in wells, multi-level redox sensors, and porewater samplers at an As-contaminated site adjacent to a freshwater tidal channel. Results indicate that sharp redox gradients exist and that redox conditions vary on tidal to seasonal timescales due to sub-daily water level fluctuations in the channel and seasonal groundwater-surface water interactions. The As and Fe^{2+} concentrations decreased during seasonal periods of net discharge to the channel. The seasonal changes were greater than tidal variations in both Eh and As concentration, indicating that impacts of the seasonal mechanism are stronger than that of sub-daily water table fluctuations. A conceptual model describing tidal and seasonal hydro-biogeochemical coupling is presented. These findings have broad implications for understanding the impacts of sea-level rise on the mobility of natural and anthropogenic coastal solutes.

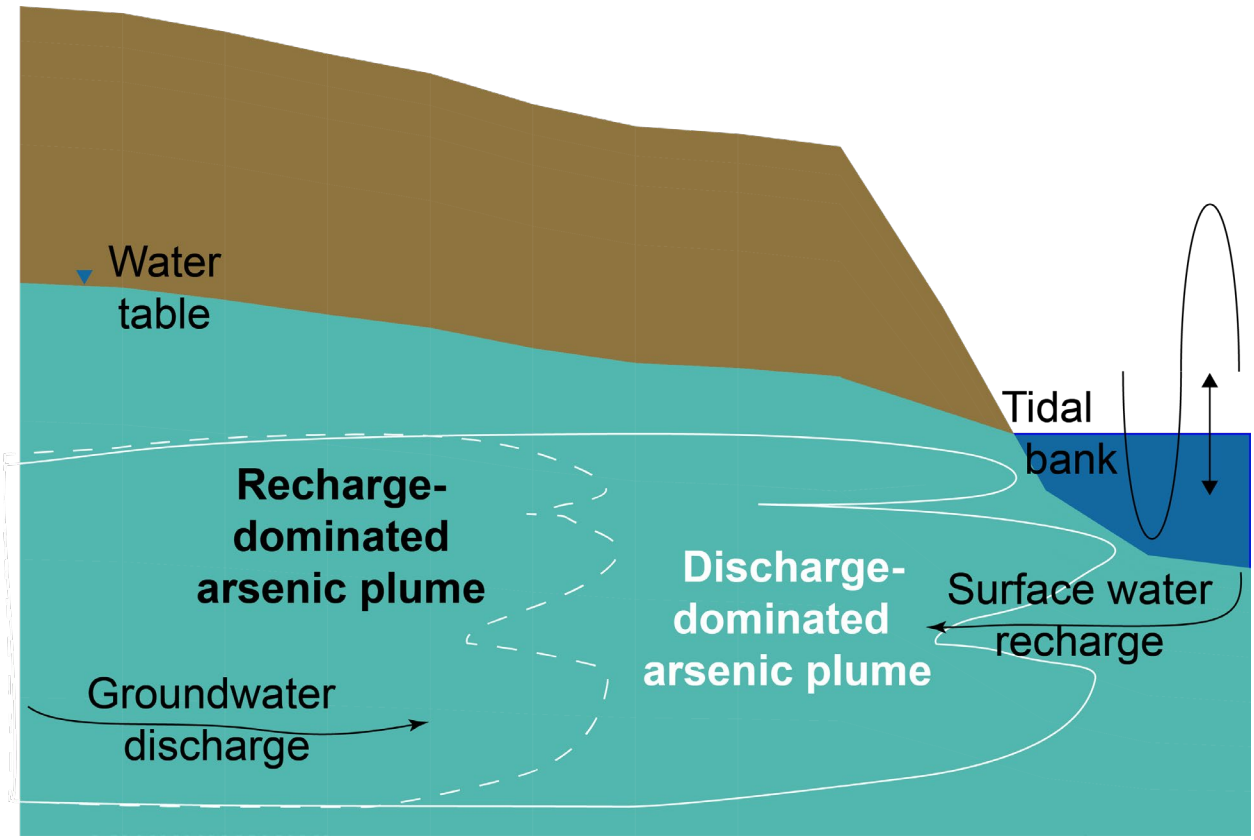
Water
table
Tidal
bank
Recharge-
dominated
arsenic plume
Discharge-
dominated
arsenic plume
Surface water
recharge
Groundwater
discharge

50

51

Accepted Manuscript
Version of record at: https://doi.org/10.1021/acs.est.2c05930

Introduction

Coastal areas contribute substantially to the well-being of people and society by supporting human livelihoods, facilitating global trade, regulating marine hazards, and providing recreational values. Yet, many industrial-contaminated soils are located along coastlines[1,2], making the nearby environment vulnerable to migration of hazardous materials. Studies have demonstrated that diverse natural processes such as flushing rates of aquifers[3], dissolution of carbonate minerals[4], and saltwater intrusion[5] control the chemical release (mobilization) of redox-sensitive species like arsenic (As) into groundwater. In addition, human activities can introduce trace metals to the coastal environment[1,6]. The mobility of hazardous materials increases pressure on coastal groundwater resources[7] and ecosystem health[8]. So, assessing vulnerability of these important areas to As contamination due to mobilization from sediments is essential for groundwater management and environmental risk mitigation[9–11].

More than three decades of research on groundwater As has laid the foundation that dynamic As cycling zones can occur at groundwater-surface water interfaces. When anoxic groundwater meets oxygenated surface water, fate and transport of As are intimately tied to the biogeochemical reactions impacted by the dynamic mixing between the two waters[12–14]. An important mechanism for As release in these reaction zones is organic carbon-driven reduction of iron minerals on which As is bound[15]. This reductive dissolution often occurs after the oxygen in infiltrated surface water containing dissolved organic carbon is consumed[16]. However, As concentrations have been shown to be highly heterogeneous in groundwater across different scales[17–20]. In addition, the relationship between the solid-phase and dissolved As is highly

variable[21–23]. Thus, it remains a challenge to unravel the factors that affect groundwater As contamination risk at local scales[15,24].

One critical uncertainty that affects the evolution of As concentration is the interplay between hydrologic and geochemical alterations across scales. The difference in wet season and dry season water fluxes between the aquifer and the river was found to be a critical controlling factor in the formation of an As reaction zone within river banks of the Ganges-Brahmaputra-Meghna Delta[25]. Heavy metal concentrations in coastal aquifers have been shown to fluctuate due to oxidation–reduction processes in response to tidal dynamics[26]. A tidally controlled redox gradient can cause porewater exchange and considerable As mobilization[27]. At a higher temporal resolution, wave-induced circulation of surface water through lake banks can form a reaction zone below the shoreline, leading to As accumulation[28]. Hydrologic shifts induced by human activity can also alter the biogeochemical reaction zone for As cycling. In the Jianghan Plain, China, As concentrations were dramatically altered by groundwater pumping due to seasonal transition between recharge and discharge, where elevated As concentration was due to reduction of As-bearing iron (Fe) minerals[29]. In the Red River flood plain near Hanoi, Vietnam, Arsenic contained in the Fe-oxides can be released during their dissolution when the floodplain aquifer was flushed[30]. More broadly, in South Asia, large-scale groundwater abstraction has been shown to alter groundwater flow paths by inducing an advective flux of surface water riverbeds to create hotspots of reactive Fe oxides, leading to As migration distances of several kilometers[15]. These diverse field settings resulted in As release and transport in response to different combinations of hydrologic and geochemical processes, indicating that the mechanism of As

release accompanying reductive iron dissolution is complex and may occur on multiple temporal and spatial scales.

In coastal industrial-contaminated sites, hydrological regimes may be substantially altered due to climate change, anthropogenic activities, and sea-level rise (SLR) [31–33]. Consequently, As cycling processes could be affected, which may require updated remediation plans[34]. Recent laboratory experiments showed that inundation of contaminated soils may release redox-sensitive hazardous materials to groundwater in future SLR scenarios[35]. The risk of redox-sensitive radionuclide technetium to be mobilized from reduced subsurface sediments during sea-level rise is different between intrusion and inundation due to different hydrologic flow velocities[31]. In a previous laboratory study[36], it was found that more As was released when the sediment was reacted with river water than with sea water. This was attributed to the higher levels of sulfur in the seawater which inhibited the reductive dissolution of ferric iron and arsenate. Also in laboratory experiments, it was revealed that geochemically trapped trace metals in the soil can be released even during low-energy resuspension events, and more than 80% release of As happens after the flooding events[37]. In environmental settings, the consequences of SLR for hydrological and geochemical shifts could be complicated due to interaction between different forcings across temporal scales, but field observations across multiple time scales of groundwater As near industry-contaminated sites are rarely reported[12,28,38]. This study collected field data to identify the hydrogeochemical conditions that are most important for controlling As cycling at industrial contaminated coastal areas. The monitoring results demonstrate the transient response of the reaction zone of As over different time scales, which have implications for understanding

impacts of groundwater-surface water interactions on contaminant mobility under future hydrological change.

Materials and Methods

Site Description

The study site is a storm water drainage ditch connected to a tidal river in Wilmington, Delaware, USA (Fig. 1a). The ditch is regularly inundated by semidiurnal tides (i.e., each transition between low to high tides lasts approximately 12 hours and 25 minutes). Net annual flow is from the aquifer to the tidal channel. The hydraulic gradient between the south bank (A) and the channel inverts tidally: during the rising tide, the flow direction is from the channel to the south bank, but during the falling tide, the flow direction is toward the channel. In addition, the river water elevation shows spring (highest monthly tidal amplitude) -neap (lowest monthly tidal amplitude) tidal cycle with a period about 14.5 days [39]. The western portion of the channel is adjacent to industrial sites which previously hosted a chemical production facility for more than 30 years and an ore processing factory (see Text S1). In recent years, elevated levels of As were detected in the channel and in the groundwater (Fig. S1), indicating contaminant plume migration.

Field instrumentation and sampling

Beginning in August 2000, monitoring wells were installed along the channel bank as part of remediation monitoring requirements. Five of those wells were selected to observe hydraulic head along the south bank. In each well, 5-foot length of 'pre-packed' Geoprobe™ well screen was placed just below the observed water table surface from approximately 2.5m. Pressure

141 transducers (Mini-Diver, Schlumberger) were placed in the wells in September 2014. Another
142 pressure transducer (Mini-Diver, Schlumberger) was placed in a slotted PVC pipe, which was
143 fixed on the bottom of the channel (Fig. 1), to measure stream stage. The atmospheric variation
144 was recorded by a Baro-Diver (Schlumberger).

145 Multilevel in-situ redox sensors (Paleo Terra, Amsterdam, Netherlands) were installed next to
146 Well 3 (Fig. 1b) after validation (see Text S2). The sensors were built from fiber glass-epoxy
147 tubes with an external diameter of 12 mm, installed vertically by hand to ensure electrodes had a
148 good connection to the sediments, and connected to dataloggers (CR1000 and AM16/32B,
149 Campbell Scientific Inc., Logan, UT, USA). Three probes (labelled as yellow, black, and red,
150 Fig. 1c) were installed next to each other, each with 10 redox-sensing platinum electrodes at 15-
151 cm intervals. The yellow probe was installed from the ground surface (0 m, as the basis) to 1.5 m
152 deep in the soil. The black probe was placed from 1.5 m to 3 m with an extension on the top. The
153 red probe was placed from 2.2 m to 3.7 m with two extensions until refusal.

154 Porewater samplers were installed with ports at different depths, co-located with the redox
155 probes. Samplers were made from push points with a stainless-steel mesh screen (AMS, Inc.,
156 American Falls, ID, USA) and installed with a removable steel push rod and hammer drill.
157 PharMed tubing (16, 1/8'' i.d., Cole Parmer, Chicago, IL, USA) was attached to the top of each
158 sampling point to facilitate sampling with a peristaltic pump. The final depths of the porewater
159 samplers were 1.75, 2.59, and 3.07 m, separately, due to the installation and the refusal from a
160 hardpan.

161 Groundwater and channel water samples were collected over a range of time scales. Spring-neap
162 cycles were captured by sampling every two or three days for two weeks (on 14, 16, 19, 22, 27,

and 30 October 2015). Seasonal cycles were captured by samples from October 2014, December 2014, Feb 2015, May 2015, October 2015, November 2015, and January 2016 –accessibility restrictions prohibited additional site access. Every sampling day, water was collected twice, at the high tide and low tide during the daytime, to examine the tidal variability of As concentration. A peristaltic pump was used to collect porewater. The initial 300 ml from each sampling port were discarded, and then the pump was immediately connected to a flow-through cell (Yellow Springs, Ohio, USA) and a YSI Professional Plus handheld multiparameter meter (Yellow Springs, Ohio, USA) to measure pH, dissolved oxygen, Eh, salinity, and temperature. Then, porewater samples were collected in acid-washed high-density polyethylene (HDPE) bottles and immediately filtered using a 0.2 μm nylon filter. Once filtered, samples were analyzed for ferrous iron (Fe^{2+}) via the phenanthroline method using field colorimetric analysis (CHEMetrics V-2000, Washington, D.C., USA). A subsample aliquot was acidified to 2% trace metal grade HNO_3 and stored at 4°C for As and Fe analysis. Because many of the reaction pathways controlling As and Fe redox reactions are microbially mediated, C and N concentrations were determined using a second filtered aliquot that was stored frozen until DOC and nitrate analysis.

Sediment from the channel bottom was collected to 20 cm depth using a 3 cm push corer on 11 Sep 2014. Soil cores from the channel bank were collected using a Geoprobe™ direct push drill with a 5 cm coring attachment and logged from the surface to 3.7 m below the surface. Once recovered, measures were taken to limit potential exposure of the core to oxidation, including immediately placing vinyl caps on the polyvinyl chloride (PVC) core sleeves and wrapping the core sleeves in polyethylene film, and transporting the cores on ice to an anaerobic chamber for storage and processing within 6 h. Total arsenic content of the sediment samples was determined

by microwave-acid digestion (US EPA 1995 Method 3051), followed by analysis via inductively coupled plasma atomic emission spectrometry (ICP-AES, Thermo Elemental Intrepid II XSP Duo View).

Laboratory analysis

To gain a greater understanding of the chemical form and oxidation state of the As in the channel sediments and the potential source sites, X-ray absorption near-edge spectroscopy (XANES) analyses were performed. A channel bottom sediment core sample was taken using a direct push corer with PVC liner and vinyl cap that was immediately applied upon core retrieval. The capped core was transported on ice to the lab and placed in an anaerobic glove bag within 6h. Once in the glove bag, samples were dried under anaerobic (95% N_2/5% H_2) atmosphere and homogenized to a fine powder, then stored in the inert atmosphere until synchrotron analyses. The inert atmosphere subsamples were then transported in oxygen-free containers to synchrotron facilities for XANES analysis (see Text S3).

Groundwater samples were transported to the University of Delaware Advanced Materials Characterization Laboratory for analysis of arsenic (As) and iron (Fe) by inductively coupled plasma mass spectrometry (for As ICP-MS, Agilent Technologies 7700 Series) or ICP-OES (for Fe). Nitrate (NO_3^-) was measured with ion chromatography (Dionex ICS 3000 with AS-18 column). Dissolved organic carbon (DOC) was measured by high temperature catalytic oxidation (Vario TOC Cube, Elementar Americas, Mt. Laurel, NJ, USA).

Hydrologic analysis

Tidal-signal attenuations were used to compute hydraulic diffusivities and estimate regional hydraulic conductivities of the site, following the Jacob-Ferris method described by Zotzoll et

al.[40]. The diffusivity of amplitude attenuation, D_{amp} can be calculated as:

$$D_{amp} = \frac{K \times b}{S} = \frac{x^2 \pi}{(\ln A)^2 \tau} \quad (1)$$

where K is the hydraulic conductivity (m day^{-1}), b is aquifer thickness (m), S is specific yield, x is distance (m), A is the ratio of amplitude of the oscillation in an observation well to amplitude of the ocean, τ is period (days) of the oscillation.

Results

Sediment characteristics

According to unpublished coring reports conducted by a private consulting firm under the direction of the United States Environmental Protection Agency (EPA) and Delaware Department of Natural Resources and Environmental Control (DNREC), the ditch bank soil was described as having four layers of soils (Fig. S2a). The first layer was stone and riprap, extending 0.5 m deep from ground surface. The second layer was a very pale brown (10YR 8/4) clay loam occurring between 0.5 and 1.1 m depth. The third layer was a dusky red (5R 3/2) sandy loam occurring from 1.1 to 1.8 m deep. The fourth layer was a very dusky red (5R 2.5/3) loamy sand.

Sediment was collected from both the bank and channel bottom for chemical analyses. Channel bottom sediment As concentrations varied from 5,244 to 13,296 mg kg^{-1}. Yellow-brown groundwater seepage was visually observed along the ditch bottom during ebb tide (Fig. S3). This groundwater seepage was verified via thermal imagery (Fig. S4). In the channel bank, the solid phase As profile suggested highly heterogeneous distribution with depth (varied from 6.6 to

2,466 mg kg^{-1}). The maximum measured concentration of solid phase As was (i.e., 2,466 mg kg^{-1}) at the depth of 1.8 m from the land surface near Well 3 (Fig. S2b).

Least squares linear combination fitting of the bulk XANES spectra show that the As in the channel bottom sediment was 90% As^{III}, with the balance comprised of As^{v} (Table S1). At the channel bank, As speciation was roughly 90% As^{V} at depths above 2.4 m, with the balance comprised of As^{III}. Below this depth, a considerable shift occurred, with As^{III} increasing to 18%, and the appearance of As-S species (realgar, α-As_4S_4, was used in the linear combination fit) making up 16% of the total As, and As^{V} accounting for 66% of the total As. Mineralogic analyses of the channel bottom sediment previously published show that the total Fe content within the near-bank sediment was 97 mg g^{-1}, with 72.25 mg g^{-1} of that identified as amorphous hydrous Fe oxides via sequential extraction.[36] Additionally, mineralogic identification via XRD showed the presence of the Fe oxides hematite and goethite, as well as scorodite (Fe-As mineral phase) and tooeleite (Fe-As-S mineral phase).[37]

The amplitudes and time lags of water level fluctuation in the wells and channel were used to estimate the hydraulic conductivity of the sediment according to eq (1). The time lags between groundwater in wells and channel water levels ranged from 0.25 to 1.25 hours, depending on the well position and tidal amplitude. The mean amplitudes attenuation of each well ranged from 0.10 to 0.21. Thus, the estimated hydraulic conductivity values showed spatial patterns depended on channel proximity. The north row of three wells (Wells 2, 3, and 4, Fig. 1) was approximately 10 m from the channel, and the estimated hydraulic conductivities were $1.2x10^{-4}$, $1.5x10^{-4}$, and $2.1x10^{-4}$ m/s for the three wells, respectively. The south row of two wells (Well 1 and 5, Fig. 1)

was approximately 30 m from the channel, and the hydraulic conductivity values were $1.1x10^{-3}$ and $6.3x10^{-4}$ m/s, respectively.

Hydrochemical variations over tidal cycles

Water level data showed reversals of flow direction between the aquifer and the channel on tidal time scales. During high tides, channel stage averaged 0.94 m higher than the water level in the wells (Fig. S5). Therefore, surface water recharged into the sediment. During low tides, the channel water averaged 0.86 m lower than the water level in the wells, and the water was discharging to the channel.

Tidal fluctuations had limited impact on As and Fe^{2+} concentrations in groundwater at different depths (Fig. S5, Table S2). At the depth of 1.75 m, As concentration varied from 1.54 μg L^{-1} to 4.57 μg L^{-1} at high tide, and from 0.99 μg L^{-1} to 4.65 μg L^{-1} at low tide. The As concentrations at high tide were greater than at low tide by 0.17 μg L^{-1} (i.e., 6.9% of the mean value in low tide, Table S2) on average (p=0.185). At the depth of 2.59 m, the As concentrations at high tide were greater than at low tide by 1259 μg L^{-1} (i.e., 85.3% of the mean value in low tide, Table S2) on average (p=0.084). At the deepest sampling point (3.07 m), greater As concentrations were found during low tides on most sampling days (except Oct 14, 2015). The As concentrations at high tide were lower than at low tide by 2343 μg L^{-1} (i.e., 9.3% of the mean value in low tide, Table S2) on average (p=0.29). Concentrations of Fe^{2+} showed similar tidal variation, which was highly correlated to As concentration (Fig. S6).

Hydrochemical variations over a neap-spring tidal cycle

The groundwater As concentrations changed gradually during the neap-spring tidal cycle. During the Oct. 2015 field sampling events, the trend showed an increase of groundwater As concentrations during neap tides and decrease during spring tides (Fig. 2). A similar pattern was observed for Fe^{2+} concentration. Eh values did not show any significant trend during the neap-spring cycle. Both neap-spring tides and semidiurnal tides impacted pH, resulting in increased pH during spring tides and decreased pH during neap tides (Fig. S7). The DO, DOC, NO_3, and NH_4 was also impacted across neap-spring cycle (Fig. S7).

Hydrochemical variations over seasons

Seasonal fluctuations in water level (e.g. E_{well1} elevation water level of Well 1) show varying intensity and extent of tidal reversals throughout the sampling period (Oct. 2014 to Jan. 2016). The hydraulic gradient between Well 1 and Well 2 was calculated and compared to the recharging time ($E_{well1}<E_{well2}$) and discharging time ($E_{well1}>E_{well2}$) for each month (Fig. 2). If the monthly total recharging time was greater than the discharging time, we defined the month as a recharge-dominated month, otherwise, it was a discharge-dominated month.

Groundwater As concentrations showed considerable seasonal variation. The As concentrations (Fig. 2) were consistently higher in recharge-dominated months (Oct 2014, Dec 2014, Oct 2015, Nov 2015) than in discharge-dominated months (Feb 2015, May 2015, Jan, 2016). This trend was especially clear in deeper groundwater, where the As concentration ranged from $1.0x10^4$ - $2.7x10^4$ μg L^{-1} (i.e. 10 - 27 ppm, parts per million) in recharge-dominated months, while the As concentration was below 200 μg L^{-1} in discharge-dominated months (Fig. 2c). Similarly, Fe^{2+} showed higher concentrations (Fig. 2d) in recharge-dominated months (mean: 377.84 mg L^{-1}; standard deviation: 100.8 mg L^{-1}) than discharge-dominated months (mean: 78.32 mg L^{-1};

297 standard deviation: 106.5 mg L^{-1}). The DO, DOC, NO_3, and NH_4 showed complex variation over
298 seasons (Fig. S8).

299 **Continuous redox cycling across different temporal scales**

300 Soil redox showed a pronounced bimodal depth profile from the surface to a depth of 3.6 m (Fig.
301 S1c). In the top (from 0 to 0.5 m deep), the soil was in an oxidized condition. From 0.5 to 1.2 m
302 deep, the redox condition fluctuated between reducing and oxidizing (Fig. S1c). The zone from
303 1.2 to 2.0 m deep was saturated at high tide and unsaturated at low tide (Fig. S1c). The Eh values
304 between 1.2 and 2.0 m reflected oxidizing conditions (i.e. Eh >150 mV) and decreased with
305 depth as the soil was more frequently saturated. The soil was always saturated below 2.0 m and
306 in a reducing condition. The variability decreased in deeper layers, except for the deepest sensor
307 (3.6 m deep. Fig. S1c).
308
309 Tidal fluctuations impacted redox variation across time. Two contrasting tidal impacts could be
310 found at different depths. From Dec. 5th to Dec. 9th, 2014, the soil redox at 2.1 m was negatively
311 correlated with the tides (Pearson correlation coefficient = -0.77, Fig. 3c). In the deeper zone (2.7
312 m), the soil redox was positively correlated with the tides (Pearson correlation coefficient = 0.88,
313 Fig. 3c). At other depths soil redox had a weaker correlation with tides.
314
315 Spring-neap cycles also impact tidal control on redox. Daily correlations between surface water
316 elevation and redox along the soil profiles showed a complex temporal variation (Fig. 3a).
317 During neap tides (Fig. 3b), more negative correlations existed between surface water elevation
318 and soil redox, whereas during spring tides, a more positive correlation was found (Fig. 3a).
319

Average redox variation showed different seasonal trends in the shallow soil and variably saturated zones. In the top layer (0-0.5m), the monthly average soil Eh increased slightly from 2014 Oct to 2016 Jan (Fig. S9c, Table S3). In the second layer (0.5-1.1 m), the soil redox changed from reducing to oxidizing conditions gradually (Fig. S9d, Table S3). The third layer was usually in an oxidizing condition, with significant increasing trends during the monitoring period (Fig. S9e, Table S3). In the bottom layer, the soil redox was uniformly low, decreasing slightly over time with no significance (Fig. S9f, Table S3).

Discussion

Hydrogeochemical factors controlling the variation of reactive zone

We observed two hydrologic factors that control redox conditions in our field site. One is the position of the water table – depths that are above or near the water table are exposed to air, resulting in higher Eh values. This suggests depths in the zone of fluctuation exhibit a negative correlation between water table elevation and Eh. This mechanism was also observed at a regularly inundated acidified site.[38] The second factor is the influence of oxic river water (see Text S4) in the aquifer near the tidal channel. The influence will extend farther into the aquifer from the bank during conditions when the aquifer is being recharged from the channel compared to conditions in which the aquifer is discharging into the channel. A similar process was found in the hyporheic zone of the Ganges-Brahmaputra-Meghna Delta[25]. Recharging conditions occur when tide is high compared to the groundwater level, and discharging conditions when tide is low (Fig. S5b). Thus, at depths below the water table, we would expect a negative correlation between hydraulic gradient and Eh. Since the gradient tends to drive groundwater discharge

during low tide and recharge during high tide, we would also expect a negative correlation between tide and Eh. This conceptualization of differing hydrologic controls on redox with depth is consistent with the observed negative correlation at 2.1m depth and the observed positive correlation at 2.7m depth. Such contrasting redox responses resulted in different effect of tide on As concentration at 2.59 m and 3.07 m (Table S2). A combination of heterogeneity in aquifer geochemical and hydrologic characteristics (i.e. hydraulic conductivity as evidenced by the tidal analysis) and complexity of flow paths may explain a lack of correlation at other depths. This conceptualization is also consistent with the observed influence of spring-neap cycles on the diurnal tidal influence. During spring tides, the hydraulic gradient is primarily driving recharge to the aquifer from the channel, whereas during neap tides, conditions were mostly discharging (Fig. 2b). This is consistent with the observation that correlations between Eh and tidal elevation become more negative during spring tides and more positive during neap tides. During the recharge dominated time, the gradients are such that the channel bank is mostly gaining (i.e. more water flows from surface to groundwater). However, the oxygenated surface water isn't getting to our measurement site (Fig. 4). The groundwater flowing from the land side is still anoxic, even during times of higher recharge. The recharge in both seasons only oxygenates the very top of the water table, which was supported by different tidal response of As concentration at the depths of 2.59 m and 3.07 m (Table S2). Over the yearly cycle, both the water table fluctuations and the direction of groundwater flow affect soil Eh, resulting in changes in both average Eh and its monthly variability (Fig. S9).

Results indicate that groundwater flowing toward the channel is reducing, with a dissolved arsenic plume originating from distal locations to the south and extending in the direction of groundwater flow to the ditch. As the reducing groundwater high in As and Fe^{2+} mixes with oxic

366 water near the bank, Eh rises and both Fe and As are immobilized onto near-bank sediment. This
367 is consistent with observations of very high solid-phase As concentrations in the channel bank
368 relative to that of sediments farther into the aquifer, and is also consistent with observations of an
369 'iron curtain' in discharge zones of coastal aquifers[25,41,42].

370 Because hydraulic gradients in this tidal system are shifting over diurnal, lunar, and seasonal
371 cycles, the plume edge is constantly accelerating and changing directions, likely resulting in
372 relatively wide Eh and As-concentration gradients. As gradients shifts landward or toward the
373 channel, the Eh values and As concentrations at the monitoring points will vary depending on the
374 magnitude of the Eh/As gradient and the magnitude and direction of advective groundwater
375 movement, which is dependent on the hydraulic gradient and proportional to hydraulic
376 conductivity. Groundwater in this system only moves on the order of centimeters over a day and
377 decimeters over a week (Fig. 4). Over the 15-month sampling period, the net movement was only
378 5 m. This supports the conceptualization that the observed variations in Eh and As concentration
379 are due to shifting of the plume edge gradients, leading to successively larger variations with
380 temporal scale of hydrologic shifts (Figs. S5 and 2). Along with advective shifts, it is likely that
381 some changes are also due to chemical reactions. For example, as more reducing groundwater
382 comes into contact with previously oxic zones, aqueous As concentrations may increase further
383 due to release from reductive dissolution of Fe.

384 The coupled hydrologic and geochemical cycling across different time scales is complex,
385 creating a heterogeneous distribution of both solid and aqueous phase As with distance from the
386 source, the ditch, and with depth[43]. Even though tidal forcing has limited impact at a single
387 observation location, the cumulative effects of transient hydrologic and geochemical processes
388 may be substantial and evolve through time[15,42].

Implications for As mobility under hydrologic change

In the long term, the hydrologic conditions and the geochemical zonation favor As accumulation in both the ditch sediment and groundwater. The As content in the sediments increased from 390 to 13,296 mg kg^{-1} in 10 years (2005-2014). The mean groundwater As concentrations also increased (Fig. S1). Multi-scale (e.g. high-tide/low tide, spring-tide/neap-tide) observation showed groundwater As fluctuations at different temporal scales. Limited groundwater samples (e.g. annual, or seasonal) may cause misinterpretation of the trends of groundwater As concentration. Such a complex mechanism of groundwater As cycling in a simple tidal environment (i.e. no significant changes in groundwater level and gradient Fig. S9a and S9b, Table S2) may be easily over-simplified if the multiscale temporal dynamics were not revealed.

Arsenic speciation in soils and sediment is impacted by redox conditions, and will therefore be altered as hydrologic conditions vary. The measured conditions at this site show that predominantly oxidizing environments lead to increased proportions of the less mobile As^{V} species compared to fluctuating redox or permanently reducing redox zones. The saturated channel bottom sediment at the point of the hydrologic seep contained very high As concentrations and is the most vulnerable to As release due to its high percentage of As^{III}. Future hydrologic shifts such as increased recharge and sea level may increase the saturation of these coastal industrially contaminated soils due to SLR or storm surge inundation. This would likely expand reducing zones in the shallow sediments, potentially increasing groundwater As risks across different time scales. Increased soil saturation will also shift variably reducing zones to become permanently saturated, which may actually decrease As mobility through sulfide mineral authigenesis. Under prolonged reducing conditions with sufficient S concentrations, As can be

removed from solution via incorporation into authigenic sulfide minerals, such as orpiment or realgar[44–46]. The channel bank's permanently saturated zone maintained redox conditions that were favorable for arsenic sulfide authigenesis. The authigenic arsenic-sulfide species present in the channel bank are relatively more stable than As^{III}, but a hydrologically-driven shift in redox conditions from reducing to oxidizing may lead to oxidative dissolution of the authigenic arsenic sulfides. This potential for oxidative and reductive dissolution of As complexes further complicates the concept of predicting contaminant mobility in future hydrologic regimes.

Under storm surge scenarios, surface water inundation can create largescale groundwater-surface interactions[47], which have been shown to increase As mobility[17]. Future SLR will introduce ocean water, which can substantially change the geochemical setting of the site[31]. Experimental and field investigations suggest that a rapid increase in salinity could drive a variety of As release mechanisms depending on the microbial inhibition of oxide dissolution[20,36].

In addition to hydrologic changes, geochemical changes may affect As cycling and thus the potential release of pollutants to surface water and groundwater. For example, continuous SLR may increase salinity of surface water in the ditch over time, which could affect the geochemical behavior of As. Hence, both hydrologic and geochemical dynamics of the ditch water should be characterized for understanding As mobility.

■ AUTHOR INFORMATION

Corresponding Author

Holly A. Michael − *Department of Earth Sciences and Department of Civil & Environmental Engineering, University of Delaware, Newark, DE 19716, United States;* orcid.org/ 0000-0003-1107-7698; Email: hmichael@udel.edu

Authors

Xuan Yu, − *Center for Water Resources and Environment, School of Civil Engineering, Sun Yat-sen University, Guangzhou, 510275, China; Southern Marine Science and Engineering Guangdong Laboratory (Zhuhai), Zhuhai, 519082, China https://orcid.org/0000-0002-9055-7923*

Joshua J. LeMonte, − *Department of Geological Sciences, Brigham Young University, Provo, UT 84602, United States*

Junxia Li, − *School of Environmental Studies & State Key Laboratory of Biogeology and Environmental Geology & Key Laboratory of Source Apportionment and Control of Aquatic Pollution, Ministry of Ecology and Environment, China University of Geosciences, 430074, Wuhan, China*

Jason W. Stuckey, − *Department of Natural Sciences and Environmental Science Program, Multnomah University, Portland, OR 97220, United States*

Donald L. Sparks, − *Department of Plant and Soil Sciences, University of Delaware, Newark, DE 19716, United States*

John G. Cargill, − *Department of Natural Resources and Environmental Control, New Castle, DE 19720, United States*

Christopher J. Russoniello − *Department of Geosciences, University of Rhode Island, Kingston, RI 02881, United States*

Accepted Manuscript
Version of record at: https://doi.org/10.1021/acs.est.2c05930

460 **Figures**

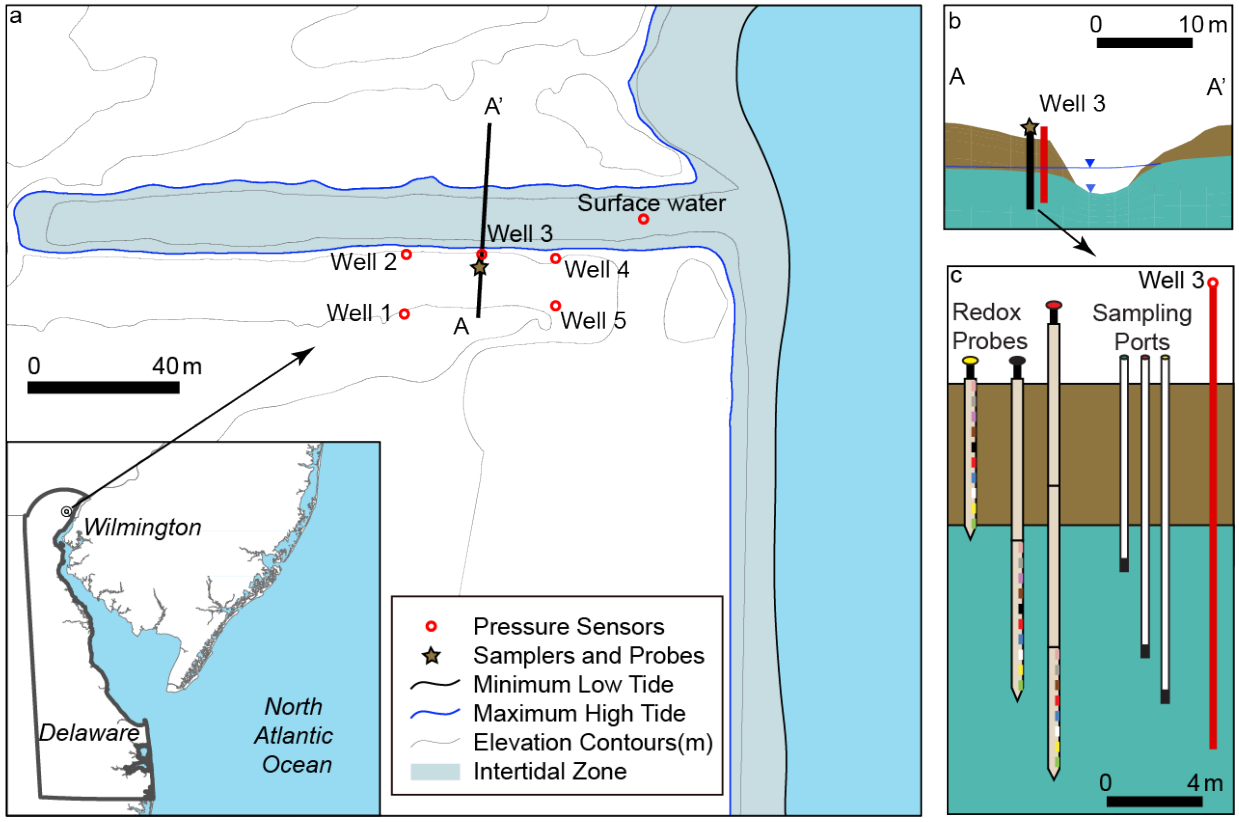

461

462 Figure 1. Tidal channel and field sampling locations. a) site map, b) A-A' cross section showing

463 sampling equipment location (black bar), and saturated zone at low (solid teal) and high (blue

464 line) tides, c) schematic of porewater sampling equipment and redox probes.

Accepted Manuscript
Version of record at: https://doi.org/10.1021/acs.est.2c05930

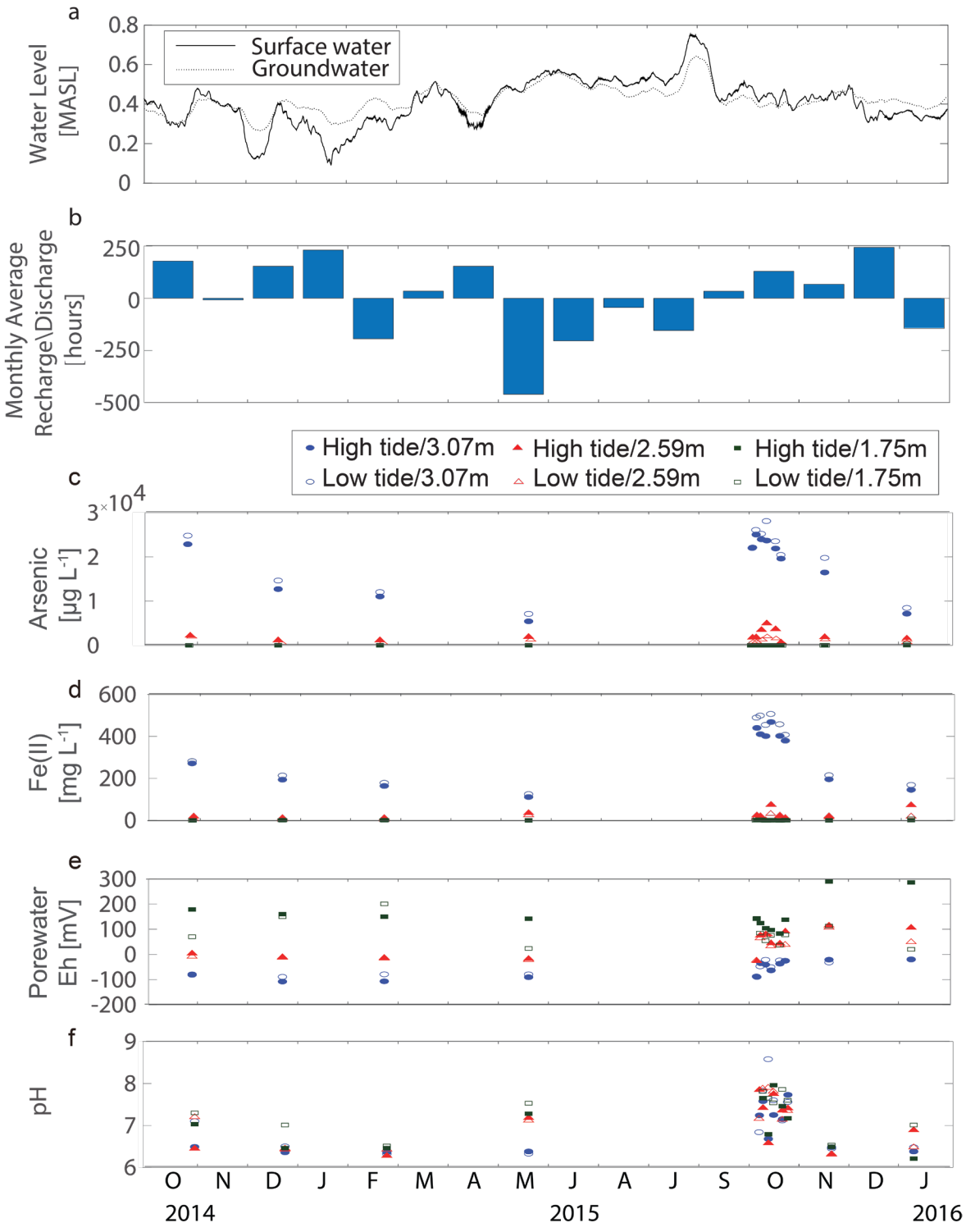

Figure 2. Seasonal fluctuation and variation of hydrochemical parameters. a) Daily surface water elevation in the ditch and groundwater elevations at Well 3. b) Cumulative recharging/ discharging hours in each month. c-f) Hydrochemical parameters of porewater samples.

Accepted Manuscript
Version of record at: https://doi.org/10.1021/acs.est.2c05930

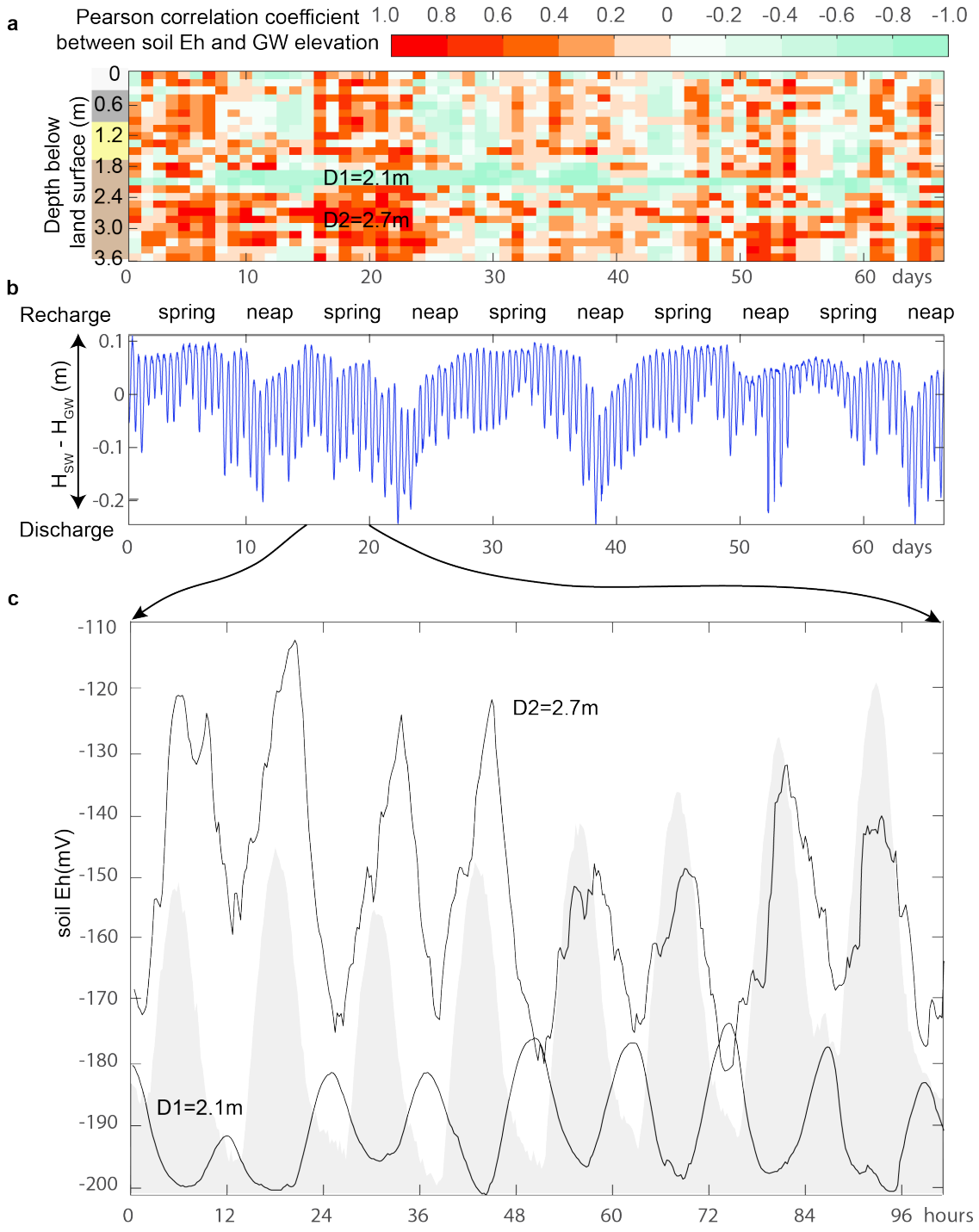

Figure 3. Sub-daily hydrologic fluctuation and soil Eh. a) The Pearson correlation coefficient between groundwater level and soil Eh every day from 2014 Nov 19th to 2015 Jan 23th. b) The difference between surface water and groundwater elevation. c) The observed 15-min soil Eh and at depths of 2.1 m and 2.7 m from 2014 Dec 5th to Dec 9th.

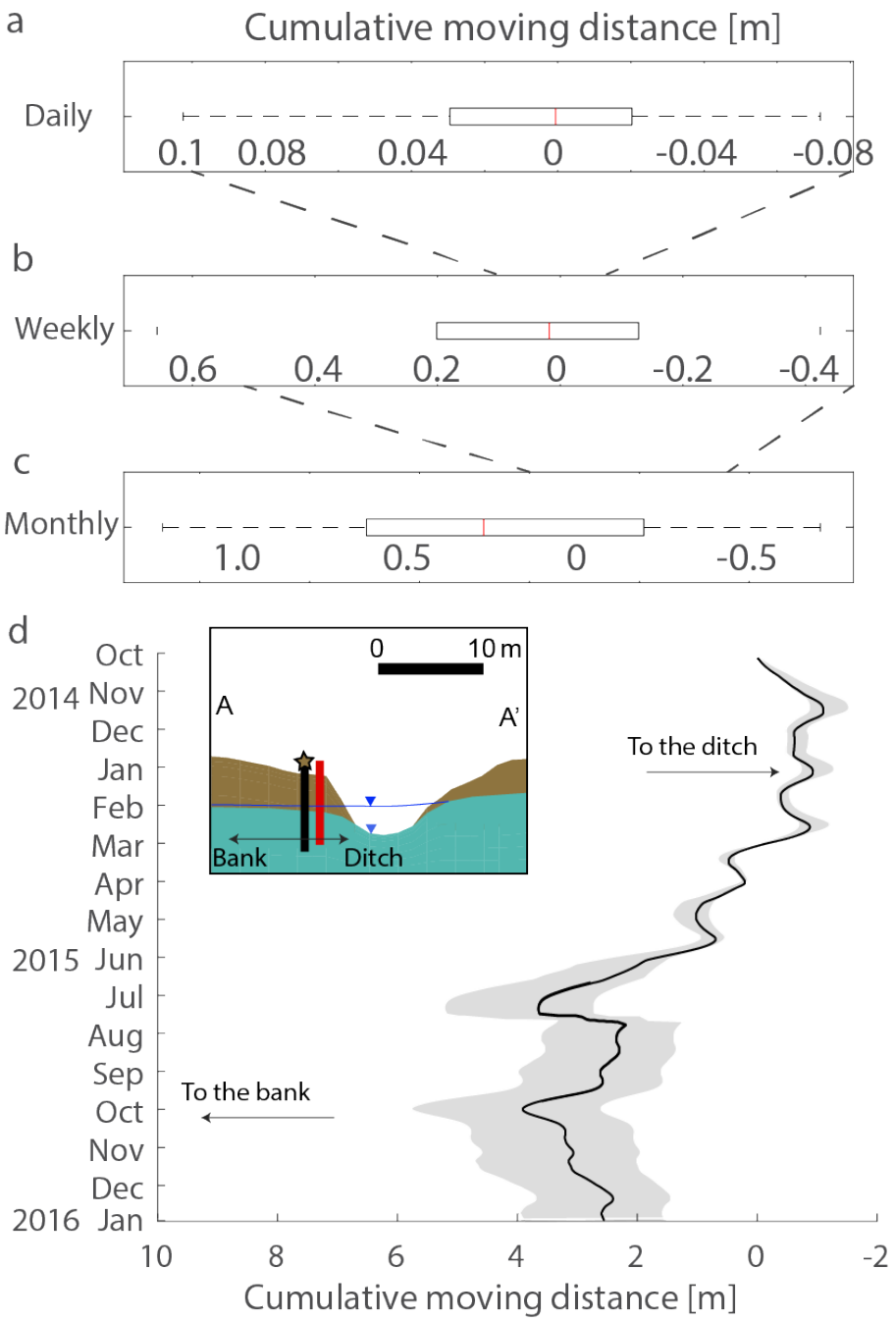

474

475 Figure 4. Hydrologic control on the movement of the As plume on a) daily, b) weekly, and c)
476 monthly timescales, with positive values indicating bankward movement. Bar plots in a-c show
477 the mean, 25-75%, and 5-95% movement for each timescale. d) black line indicates mean, and
478 grey region indicates 25-75%. The insert is Figure 1b to show the direction of ditch and band.

479

ASSOCIATED CONTENT

SI Supporting Information

The Supporting Information is available free of charge at Remediation activities (Text S1); validation of redox probes (Text S2); XANES Spectroscopy analysis (Text S3); River water chemistry (Text S4); XANES data (Table S1); As concentration fluctuation due to tides (Table S2); Observed monthly trends in water table and soil Eh (Table S3); yearly As concentration trend (Figure S1); profiles of sediment, As, and soil Eh (Figure S2); image of iron precipitation (Figure S3); thermal imagery of groundwater seepage (Figure S4); tidal fluctuation and variation of hydrochemical parameters (Figure S5); As concentration correlates with Fe^{2+} concentration (Figure S6); tidal fluctuation and variation of DO, DOC, NO_3, and NH_4. (Figure S7); hydrochemical parameters at the seasonal scales (Figure S8); seasonal hydrologic fluctuation and soil Eh (Figure S9).

ACKNOWLEDGMENTS

The authors thank Rich Landis from DuPont for help with probe installation. Gerald Hendricks and Caroline Golt provided laboratory assistance. Steve Hicks provided technical support for data logger installation. This work was supported by the National Science Foundation EPSCoR Grant No. IIA-1301765 and the Guangdong Provincial Department of Science and Technology, China Grant No. 2019ZT08G090

REFERENCES

(1) Baeyens, W.; Mirlean, N.; Bundschuh, J.; de Winter, N.; Baisch, P.; da Silva Júnior, F. M. R.; Gao, Y. Arsenic Enrichment in Sediments and Beaches of Brazilian Coastal Waters: A Review. *Sci. Total Environ.* **2019**, *681*, 143–154. https://doi.org/10.1016/j.scitotenv.2019.05.126.

(2) Liu, X.; Zeng, B.; Lin, G. Arsenic (As) Contamination in Sediments from Coastal Areas of China. *Mar. Pollut. Bull.* **2022**, *175*, 113350. https://doi.org/10.1016/j.marpolbul.2022.113350.

(3) van Geen, A.; Zheng, Y.; Goodbred, S.; Horneman, A.; Aziz, Z.; Cheng, Z.; Stute, M.; Mailloux, B.; Weinman, B.; Hoque, M. A.; Seddique, A. A.; Hossain, M. S.; Chowdhury, S. H.; Ahmed, K. M. Flushing History as a Hydrogeological Control on the Regional Distribution of Arsenic in Shallow Groundwater of the Bengal Basin. *Environ. Sci. Technol.* **2008**, *42* (7), 2283–2288. https://doi.org/10.1021/es702316k.

(4) Amarathunga, U.; Diyabalanage, S.; Bandara, U. G. C.; Chandrajith, R. Environmental Factors Controlling Arsenic Mobilization from Sandy Shallow Coastal Aquifer Sediments in the Mannar Island, Sri Lanka. *Appl. Geochem.* **2019**, *100*, 152–159. https://doi.org/10.1016/j.apgeochem.2018.11.011.

(5) Colombani, N.; Mastrocicco, M.; Prommer, H.; Sbarbati, C.; Petitta, M. Fate of Arsenic, Phosphate and Ammonium Plumes in a Coastal Aquifer Affected by Saltwater Intrusion. *J. Contam. Hydrol.* **2015**, *179*, 116–131. https://doi.org/10.1016/j.jconhyd.2015.06.003.

(6) Luo, M.; Zhou, C.; Ma, T.; Guo, W.; Percival, L.; Baeyens, W.; Gao, Y. Anthropogenic Activities Influence the Mobilization of Trace Metals and Oxyanions in Coastal Sediment Porewaters. *Sci. Total Environ.* **2022**, *839*, 156353. https://doi.org/10.1016/j.scitotenv.2022.156353.

(7) Michael, H. A.; Post, V. E.; Wilson, A. M.; Werner, A. D. Science, Society, and the Coastal Groundwater Squeeze. *Water Resour. Res.* **2017**, *53* (4), 2610–2617.

(8) Zhang, H.; Moffett, K. B.; Windham-Myers, L.; Gorelick, S. M. Hydrological Controls on Methylmercury Distribution and Flux in a Tidal Marsh. *Environ. Sci. Technol.* **2014**, *48* (12), 6795–6804. https://doi.org/10.1021/es500781g.

(9) Khan, M. R.; Koneshloo, M.; Knappett, P. S.; Ahmed, K. M.; Bostick, B. C.; Mailloux, B. J.; Mozumder, R. H.; Zahid, A.; Harvey, C. F.; Van Geen, A. Megacity Pumping and Preferential Flow Threaten Groundwater Quality. *Nat. Commun.* **2016**, *7*, 12833.

(10) Natasha; Bibi, I.; Shahid, M.; Niazi, N. K.; Younas, F.; Naqvi, S. R.; Shaheen, S. M.; Imran, M.; Wang, H.; Hussaini, K. M.; Zhang, H.; Rinklebe, J. Hydrogeochemical and Health Risk Evaluation of Arsenic in Shallow and Deep Aquifers along the Different Floodplains of Punjab, Pakistan. *J. Hazard. Mater.* **2021**, *402*, 124074. https://doi.org/10.1016/j.jhazmat.2020.124074.

(11) Smith, R.; Knight, R.; Fendorf, S. Overpumping Leads to California Groundwater Arsenic Threat. *Nat. Commun.* **2018**, *9* (1), 2089. https://doi.org/10.1038/s41467-018-04475-3.

(12) Rakhimbekova, S.; O'Carroll, D. M.; Robinson, C. E. Occurrence of Arsenic in Nearshore Aquifers Adjacent to Large Inland Lakes. *Environ. Sci. Technol.* **2021**, *55* (12), 8079–8089. https://doi.org/10.1021/acs.est.1c02326.

(13) Bone, S. E.; Gonneea, M. E.; Charette, M. A. Geochemical Cycling of Arsenic in a Coastal Aquifer. *Environ. Sci. Technol.* **2006**, *40* (10), 3273–3278. https://doi.org/10.1021/es052352h.

(14) Rakhimbekova, S.; O'Carroll, D. M.; Andersen, M. S.; Wu, M. Z.; Robinson, C. E. Effect of Transient Wave Forcing on the Behavior of Arsenic in a Nearshore Aquifer. *Environ. Sci. Technol.* **2018**, *52* (21), 12338–12348. https://doi.org/10.1021/acs.est.8b03659.

(15) Wallis, I.; Prommer, H.; Berg, M.; Siade, A. J.; Sun, J.; Kipfer, R. The River–Groundwater Interface as a Hotspot for Arsenic Release. *Nat. Geosci.* **2020**, *13* (4), 288–295. https://doi.org/10.1038/s41561-020-0557-6.

(16) Peiffer, S.; Kappler, A.; Haderlein, S. B.; Schmidt, C.; Byrne, J. M.; Kleindienst, S.; Vogt, C.; Richnow, H. H.; Obst, M.; Angenent, L. T.; Bryce, C.; McCammon, C.; Planer-Friedrich, B. A Biogeochemical–Hydrological Framework for the Role of Redox-Active Compounds in Aquatic Systems. *Nat. Geosci.* **2021**, *14* (5), 264–272. https://doi.org/10.1038/s41561-021-00742-z.

(17) Connolly, C. T.; Stahl, M. O.; DeYoung, B. A.; Bostick, B. C. Surface Flooding as a Key Driver of Groundwater Arsenic Contamination in Southeast Asia. *Environ. Sci. Technol.* **2022**, *56* (2), 928–937. https://doi.org/10.1021/acs.est.1c05955.

(18) Yang, Q.; Jung, H. B.; Culbertson, C. W.; Marvinney, R. G.; Loiselle, M. C.; Locke, D. B.; Cheek, H.; Thibodeau, H.; Zheng, Y. Spatial Pattern of Groundwater Arsenic Occurrence and Association with Bedrock Geology in Greater Augusta, Maine. *Environ. Sci. Technol.* **2009**, *43* (8), 2714–2719. https://doi.org/10.1021/es803141m.

(19) Kao, Y.-H.; Wang, S.-W.; Maji, S. K.; Liu, C.-W.; Wang, P.-L.; Chang, F.-J.; Liao, C.-M. Hydrochemical, Mineralogical and Isotopic Investigation of Arsenic Distribution and Mobilization in the Guandu Wetland of Taiwan. *J. Hydrol.* **2013**, *498*, 274–286. https://doi.org/10.1016/j.jhydrol.2013.06.009.

(20) Northrup, K.; Capooci, M.; Seyfferth, A. L. Effects of Extreme Events on Arsenic Cycling in Salt Marshes. *J. Geophys. Res. Biogeosciences* **2018**, *123* (3), 1086–1100. https://doi.org/10.1002/2017JG004259.

(21) Islam, F. S.; Gault, A. G.; Boothman, C.; Polya, D. A.; Charnock, J. M.; Chatterjee, D.; Lloyd, J. R. Role of Metal-Reducing Bacteria in Arsenic Release from Bengal Delta Sediments. *Nature* **2004**, *430* (6995), 68–71. https://doi.org/10.1038/nature02638.

(22) Stahl, M. O.; Harvey, C. F.; van Geen, A.; Sun, J.; Thi Kim Trang, P.; Mai Lan, V.; Mai Phuong, T.; Hung Viet, P.; Bostick, B. C. River Bank Geomorphology Controls Groundwater Arsenic Concentrations in Aquifers Adjacent to the Red River, Hanoi Vietnam. *Water Resour. Res.* **2016**, *52* (8), 6321–6334. https://doi.org/10.1002/2016WR018891.

(23) Stuckey, J. W.; Schaefer, M. V.; Kocar, B. D.; Benner, S. G.; Fendorf, S. Arsenic Release Metabolically Limited to Permanently Water-Saturated Soil in Mekong Delta. *Nat. Geosci.* **2016**, *9* (1), 70–76. https://doi.org/10.1038/ngeo2589.

(24) Borch, T.; Kretzschmar, R.; Kappler, A.; Cappellen, P. V.; Ginder-Vogel, M.; Voegelin, A.; Campbell, K. Biogeochemical Redox Processes and Their Impact on Contaminant Dynamics. *Environ. Sci. Technol.* **2010**, *44* (1), 15–23. https://doi.org/10.1021/es9026248.

(25) Jung, H. B.; Zheng, Y.; Rahman, M. W.; Rahman, M. M.; Ahmed, K. M. Redox Zonation and Oscillation in the Hyporheic Zone of the Ganges-Brahmaputra-Meghna Delta: Implications for the Fate of Groundwater Arsenic during Discharge. *Appl. Geochem.* **2015**, *63*, 647–660.

(26) Kumar, P.; Tsujimura, M.; Nakano, T.; Minoru, T. The Effect of Tidal Fluctuation on Ground Water Quality in Coastal Aquifer of Saijo Plain, Ehime Prefecture, Japan. *Desalination* **2012**, *286*, 166–175. https://doi.org/10.1016/j.desal.2011.11.017.

(27) Liu, S.; Tan, B.; Dai, C.; Lou, S.; Tao, A.; Zhong, G. Geochemical Characterization and Heavy Metal Migration in a Coastal Polluted Aquifer Incorporating Tidal Effects: Field Investigation in Chongming Island, China. *Environ. Sci. Pollut. Res.* **2015**, *22* (24), 20101–20113.

(28) Lee, J.; Robinson, C.; Couture, R.-M. Effect of Groundwater–Lake Interactions on Arsenic Enrichment in Freshwater Beach Aquifers. *Environ. Sci. Technol.* **2014**, *48* (17), 10174–10181.

(29) Schaefer, M. V.; Ying, S. C.; Benner, S. G.; Duan, Y.; Wang, Y.; Fendorf, S. Aquifer Arsenic Cycling Induced by Seasonal Hydrologic Changes within the Yangtze River Basin. *Environ. Sci. Technol.* **2016**, *50* (7), 3521–3529.

(30) Postma, D.; Larsen, F.; Minh Hue, N. T.; Duc, M. T.; Viet, P. H.; Nhan, P. Q.; Jessen, S. Arsenic in Groundwater of the Red River Floodplain, Vietnam: Controlling Geochemical Processes and Reactive Transport Modeling. *Geochim. Cosmochim. Acta* **2007**, *71* (21), 5054–5071. https://doi.org/10.1016/j.gca.2007.08.020.

(31) Eagling, J.; Worsfold, P. J.; Blake, W. H.; Keith-Roach, M. J. Mobilization of Technetium from Reduced Sediments under Seawater Inundation and Intrusion Scenarios. *Environ. Sci. Technol.* **2012**, *46* (21), 11798–11803.
(32) Jacobson, G. L.; Norton, S. A.; Grimm, E. C.; Edgar, T. Changing Climate and Sea Level Alter Hg Mobility at Lake Tulane, Florida, US. *Environ. Sci. Technol.* **2012**, *46* (21), 11710–11717.
(33) Sugawara, K.; Kobayashi, A.; Endo, G.; Hatayama, M.; Inoue, C. Evaluation of the Effectiveness and Salt Stress of Pteris Vittata in the Remediation of Arsenic Contamination Caused by Tsunami Sediments. *J. Environ. Sci. Health Part A* **2014**, *49* (14), 1631–1638.
(34) Sbarbati, C.; Barbieri, M.; Barron, A.; Bostick, B.; Colombani, N.; Mastrocicco, M.; Prommer, H.; Passaretti, S.; Zheng, Y.; Petitta, M. Redox Dependent Arsenic Occurrence and Partitioning in an Industrial Coastal Aquifer: Evidence from High Spatial Resolution Characterization of Groundwater and Sediments. *Water* **2020**, *12* (10). https://doi.org/10.3390/w12102932.
(35) LeMonte, J.; Stuckey, J.; Yu, X.; Rinklebe, J.; Tappero, R.; Michael, H. A.; Sparks, D. Influence of Sea Level Rise on Arsenic Mobility in Coastal Soils; 251st American Chemical Society National Meeting, San Diego, CA, 2016.
(36) LeMonte, J. J.; Stuckey, J. W.; Sanchez, J. Z.; Tappero, R.; Rinklebe, J.; Sparks, D. L. Sea Level Rise Induced Arsenic Release from Historically Contaminated Coastal Soils. *Environ. Sci. Technol.* **2017**, *51* (11), 5913–5922. https://doi.org/10.1021/acs.est.6b06152.
(37) Izaditame, F.; Siebecker, M. G.; Sparks, D. L. Sea-Level-Rise-Induced Flooding Drives Arsenic Release from Coastal Sediments. *J. Hazard. Mater.* **2022**, *423*, 127161. https://doi.org/10.1016/j.jhazmat.2021.127161.
(38) Johnston, S. G.; Keene, A. F.; Burton, E. D.; Bush, R. T.; Sullivan, L. A.; McElnea, A. E.; Ahern, C. R.; Smith, C. D.; Powell, B.; Hocking, R. K. Arsenic Mobilization in a Seawater Inundated Acid Sulfate Soil. *Environ. Sci. Technol.* **2010**, *44* (6), 1968–1973.
(39) Lee, S. B.; Li, M.; Zhang, F. Impact of Sea Level Rise on Tidal Range in Chesapeake and Delaware Bays. *J. Geophys. Res. Oceans* **2017**, *122* (5), 3917–3938. https://doi.org/10.1002/2016JC012597.
(40) Rotzoll, K.; Gingerich, S. B.; Jenson, J. W.; El-Kadi, A. I. Estimating Hydraulic Properties from Tidal Attenuation in the Northern Guam Lens Aquifer, Territory of Guam, USA. *Hydrogeol. J.* **2013**, *21* (3), 643–654.
(41) Charette, M. A.; Sholkovitz, E. R. Oxidative Precipitation of Groundwater-Derived Ferrous Iron in the Subterranean Estuary of a Coastal Bay. *Geophys. Res. Lett.* **2002**, *29* (10), 85-1-85–4. https://doi.org/10.1029/2001GL014512.
(42) Jung, H. B.; Charette, M. A.; Zheng, Y. Field, Laboratory, and Modeling Study of Reactive Transport of Groundwater Arsenic in a Coastal Aquifer. *Environ. Sci. Technol.* **2009**, *43* (14), 5333–5338. https://doi.org/10.1021/es900080q.
(43) Kumar, N.; Noël, V.; Planer-Friedrich, B.; Besold, J.; Lezama-Pacheco, J.; Bargar, J. R.; Brown, G. E.; Fendorf, S.; Boye, K. Redox Heterogeneities Promote Thioarsenate Formation and Release into Groundwater from Low Arsenic Sediments. *Environ. Sci. Technol.* **2020**, *54* (6), 3237–3244. https://doi.org/10.1021/acs.est.9b06502.
(44) Burton, E. D.; Johnston, S. G.; Kocar, B. D. Arsenic Mobility during Flooding of Contaminated Soil: The Effect of Microbial Sulfate Reduction. *Environ. Sci. Technol.* **2014**, *48* (23), 13660–13667. https://doi.org/10.1021/es503963k.

(45) O'Day, P. A.; Vlassopoulos, D.; Root, R.; Rivera, N. The Influence of Sulfur and Iron on Dissolved Arsenic Concentrations in the Shallow Subsurface under Changing Redox Conditions. *Proc. Natl. Acad. Sci.* **2004**, *101* (38), 13703–13708. https://doi.org/10.1073/pnas.0402775101.

(46) Guo, H.; Zhou, Y.; Jia, Y.; Tang, X.; Li, X.; Shen, M.; Lu, H.; Han, S.; Wei, C.; Norra, S.; Zhang, F. Sulfur Cycling-Related Biogeochemical Processes of Arsenic Mobilization in the Western Hetao Basin, China: Evidence from Multiple Isotope Approaches. *Environ. Sci. Technol.* **2016**, *50* (23), 12650–12659. https://doi.org/10.1021/acs.est.6b03460.

(47) Yu, X.; Yang, J.; Graf, T.; Koneshloo, M.; O'Neal, M. A.; Michael, H. A. Impact of Topography on Groundwater Salinization Due to Ocean Surge Inundation. *Water Resour. Res.* **2016**. https://doi.org/10.1002/2016WR018814.